



# Geochemistry of bentonitized tuff band of outer NW Himalaya, Jammu and Kashmir, India

SOM NATH KUNDAL<sup>1,\*</sup>, NIGHAT CHOWDHARY<sup>1</sup> and SANDEEP KUMAR<sup>2</sup>

<sup>1</sup>Department of Geology, University of Jammu, Jammu 180 006, India.

<sup>2</sup>Department of Geology, Cluster University of Jammu, Jammu 180 001, India.

\*Corresponding author. e-mail: snkundal123@yahoo.com

MS received 9 April 2021; revised 8 November 2021; accepted 14 November 2021

Bentonitized tuff band occur as detached outcrops in the Siwalik of northwest Himalaya in India and Pakistan at various localities with similar strikes. In Jammu province, these detached outcrops are exposed at 21 sites and Badakhetar outcrop is the thickest among all these exposed sites. The aim of the present study is to understand the nature and source of this bentonitized tuff band. Bentonitized tuff samples have been collected from Badakhetar bentonitized tuff section and analysed by XRF and ICPMS. All samples considerably have high SiO<sub>2</sub> content (59.92–72.05 wt%) than other oxides [Na<sub>2</sub>O (0.09–1.88 wt%), MgO (0.76–4.67%), Al<sub>2</sub>O<sub>3</sub> (11.73–23.88%), P<sub>2</sub>O<sub>5</sub> (0.00–0.07%), K<sub>2</sub>O (0.07–4.29%), CaO (1.27–2.03%), TiO<sub>2</sub> (0.06–0.10%), Fe<sub>2</sub>O<sub>3</sub> (0.84–3.39%)] indicating intermediate to felsic nature of the Badakhetar bentonitized tuff band and have rhyodacite to trachyandesite composition. TiO<sub>2</sub>/Al<sub>2</sub>O<sub>3</sub> values ranging from 0.0001 to 0.0230 suggest that there is no effect of weathering during the deposition of bentonitized tuff band.

**Keywords.** Bentonitized tuff band; geochemistry; XRF; Upper Siwalik Subgroup; Jammu Province.

## 1. Introduction

Bentonite deposits throughout the world occur either by diagenetic or hydrothermal alteration of pyroclastics of intermediate to acidic character (Christidis *et al.* 1995; Christidis and Dunham 1997; Christidis and Scott 1997; Christidis 1998; Yalcin and Gumuser 2000; Caballero *et al.* 2005; Ddani *et al.* 2005; Arslan *et al.* 2006; Christidis and Huff 2009). Bentonite has been successfully applied in stratigraphy as perfect time markers horizon for correlation. During the last three decades, numerous works have been carried out worldwide on bentonite geochemistry (MacDonald 1987; McLennan 1989, 2001; Barr and Cooper 2013; Batchelor 2014; Kipli *et al.* 2015; Pozo *et al.* 2016; Göncüoğlu *et al.* 2016; Elliott *et al.* 2018; Ge *et al.* 2019; Siritongkham *et al.* 2020).

The bentonite occurring in the Sub-Himalayan rocks represents an invaluable time marker horizon in the Siwalik. There is extensive literature on the volcanic ash beds of Himalayas and their tectonic settings (Middlemiss 1930; Bhola 1948; Johnson *et al.* 1982; Arif *et al.* 2005; Bhat *et al.* 2008; Ullah *et al.* 2020). From time to time volcanic ash beds/bentonite beds have been reported and studied from many places of the Siwalik Group (Visser and Johnson 1978; Opdyke *et al.* 1979; Johnson *et al.* 1982; Tandon and Kumar 1984; Burbank and Tahirkheli 1985; Bhat *et al.* 2008).

The bentonite/bentonitized tuff band exposed in the Upper Siwalik Subgroup of Jammu was reported about 60 yrs back and their geochemistry, geochronology and depositional origin are well studied (Tripathi 1986; Yokoyama *et al.* 1987;

Ranga Rao *et al.* 1988; Mehta *et al.* 1993; Gupta 1996a, b, 2000, 2001; Gupta *et al.* 1999; Kundal *et al.* 1999, 2011; Gupta and Kochhar 2002; Bhat *et al.* 2008). However, these authors have not described the exact level (bottom, middle, top) of bentonite sampled in their studies as the bentonite bed is 3.6 m thick at Badakhetar. The bentonite bands occurring in Siwalik of Jammu area are exposed at 21 sites. Among these 21 sites, we carried out sampling only from Badakhetar site (figure 1) as the Badakhetar exposure is thickest of all. The aim of the present work is to know the nature and source of bentonitized tuff band of Siwalik of Jammu area.

### 1.1 Stratigraphy of the study area

Stratigraphically, the Siwalik Subgroup was divided into seven formations, viz., Kamliak and Chinji (Lower Siwalik Subgroup), Nagri and Dhokpathan (Middle Siwalik Subgroup) and Tatrot, Pinjor and Boulder Conglomerate (Upper Siwalik Subgroup) by Pilgrim (1934). In Jammu, all seven formations of the Siwalik are well exposed in the study area. Ranga Rao *et al.* (1988) classified the rocks of Upper Siwalik Subgroup of Jammu into Purmandal Sandstone (=Tatrot Formation), Nagrota Formation (=Pinjor Formation) and Tawi Conglomerate (=Boulder Conglomerate). Agarwal *et al.* (1993) accepted the classification of Ranga Rao and classified the Nagrota Formation into three members, viz., Nagrota Member A(NA), Nagrota Member B(NB) and Nagrota Member C(NC). Gupta and Verma (1988) classified the Siwalik rocks of Jammu into five formations, viz., Mansar Formation (Lower Siwalik Subgroup), Dewal Formation and Mohargarh Formation (Middle Siwalik Subgroup) and Uttarbaini and Dughor formations (Upper Siwalik Subgroup). Gupta (2000) refined his classification and divided the Mansar Formation into Dodenal Member and Ramnagar Member and Uttarbaini Formation into Labli Member and Marikhui Member. Recently, Elias *et al.* (2017) classified the Siwalik Group of Jammu province into six formations, viz., Mansar Formation (Lower Siwalik Subgroup), Dewal and Mohargarh formations (Middle Siwalik Subgroup) and Labli Formation, Marikhui Formation and Dughor Formation (Upper Siwalik Subgroup). The comparative up-to-date lithostratigraphic classification of Jammu Siwalik is given in table 1. The bentonite samples in the present study have been collected

from the Nagrota Member-B of Nagrota Formation (Agarwal *et al.* 1993; Ranga Rao *et al.* 1988)/Pinjor Formation (Pilgrim 1934)/Labli Member of Uttarbaini Formation (Gupta and Verma 1988)/Marikhui Formation (Elias *et al.* 2017) for geochemical analysis. The field photograph of bentonitized tuff band of Badakhetar section is given in figure 2.

### 1.2 Field observations and age of bentonitized tuff band

The bentonitized tuff bands (BTB) are persistent laterally occurring in detached outcrops for about 70 km and are embedded in mudstone–siltstone horizons. These detached outcrops of bentonitized tuff bands were reported at 21 sites in the Upper Siwalik Subgroup of Jammu. The Badakhetar bentonitized tuff band is the thickest (3.6 m) among the reported sites and is exposed 375 m northwest of village Badakhetar. The associated mudstones yielding a diverse type of micro-fauna and flora include rodents, lizards, fishes, ostracodes, gastropods and charophytes (Prasad *et al.* 2005; Bhandari and Kundal 2008; Kundal 2013, 2015, 2018; Kundal *et al.* 2017). The bentonitized tuff band is mainly composed of three types of sediments: (1) Dark gray tuffaceous mudstone, (2) Cream-coloured bentonite having high swelling property, and (3) White coloured, powdery and sandy bentonite clay having little swelling nature. Dip of the bentonitized tuff beds and the associated strata varies between 15° to 23° SW in the study section. The bentonitized tuff band generally shows sharp basal contact with the underlying mudstones and gradational contact with the overlying siltstone. The bentonitized tuff band units are internally composed of many sub-units and exhibit diverse type of sedimentary structures. These structures include graded bedding, planar- and wavy lamination, crossed bedding, load and flame structures, convolute bedding, oscillation ripples, bioturbation, pinch and swell structure and escape burrows (vertical and inclined). The cream colour bentonite shows maximum plasticity, high jel value index and high swelling properties as compared to other two varieties. The bed exhibits diffused internal stratification, picked out by subtle, variation in grain size and sorting, which is typical of many air fall deposits (Fisher and Schminke 1984). Both normal and inverse grading are common, but normal

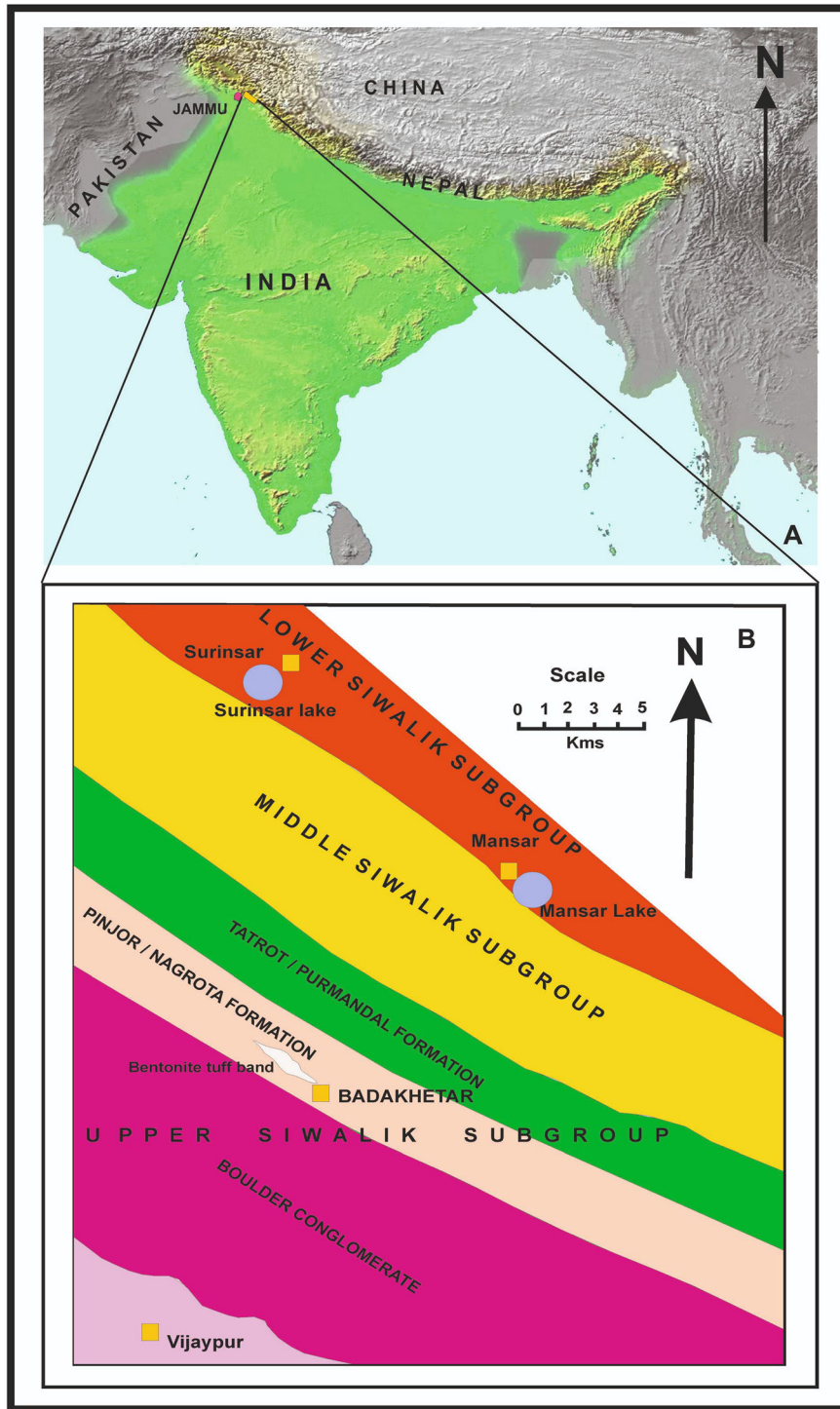


Figure 1. (A) Major tectonic units of Himalaya (after Sorkhabi and Macfarlane 1999) and (B) Bentonitized tuff band exposure in the Pinjor Formation/Nagrota Formation, Upper Siwalik of Jammu province (modified after Gupta and Verma 1988).

grading dominates. In a few beds, a rhythmic pattern exists, indicating that stratification is the product of a succession of discrete layers of tuff separated by discrete bedding planes. Moreover, the beds and laminae are naturally grouped into bedsets (e.g., predominantly fine-grained tuff and

successive graded packages) suggesting that the tuff was emplaced by multiple episodic eruptions. The change in colour from bottom to top in different laminae also indicates episodic eruption. The dark gray beds of tuffaceous bentonitized tuff band contain heavy minerals such as biotite, zircon,

Table 1. Comparative lithostratigraphic classification of Siwalik Province of Jammu.

GROUP	Siwalik Subgroups	Potwar Plateau (Pilgrim 1934)	Jammu and Kashmir (Gupta and Verma 1988)	Jammu and Kashmir (Ranga Rao et al. 1988)	Jammu and Kashmir (Agarwal et al. 1993)	Jammu and Kashmir (Eliyas et al. 2017)	Himachal Pradesh (Verma et al. 2002)	Age
SIWALIK	Upper Siwalik	SOAN FORMATION	Dughor Formation	Tawi Conglomerate	Dughor Formation	Kalar	Middle Pleistocene	
		Lower	UTTARBAINI	Nagrota Formation	Nagrota Member A	Pinjor Formation	Early Pleistocene to Late Pliocene	
		Boulder Conglomerate	Marikhui Member		Nagrota Member B			
		Pinjor Formation	Labli Member	Purmandal Sandstone	Nagrota Member C	Saketi Formation	Late Pliocene	
		Tatrot Formation						
		Formation						
Middle Siwalik		Dhokpathan Formation	Mohargarh Formation		Mohargarh Formation	Mohargarh Formation	Middle Pliocene	
		Nagri Formation	Dewal Formation		Dewal Formation	Dewal Formation	Lower Pliocene	
Lower Siwalik		Chinji Formation	Mansar Formation		Mansar Formation	Nahan Formation	Middle to Late Miocene	
		Kamlial Formation						

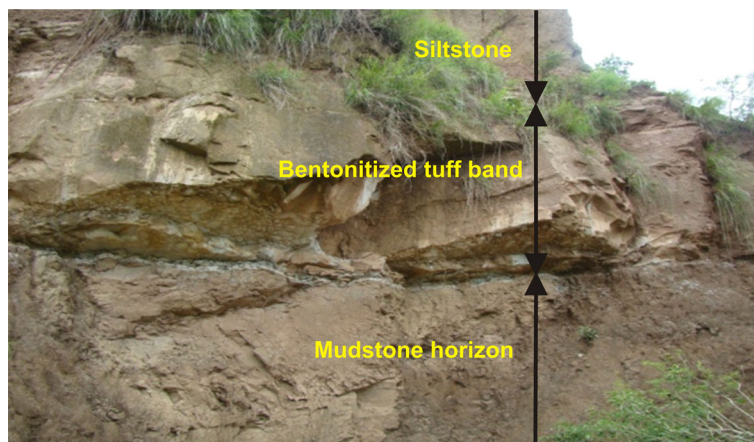


Figure 2. Field photograph showing bentonitized tuff band of Badakhetar section.

apatite, epidote, etc., and white/pinkish colour beds contain light-coloured minerals such as glass shards, quartz, feldspars, etc. Bhat *et al.* (2008) inferred four palaeolakes in the study area based on the facies studies of the bentonitized tuff band and associated mudstones. The recovery of fauna and flora underlying and overlying mudstone horizons indicates a interfluvial–lacustrine depositional environment of the study area (Bhat *et al.* 2008; Bhandari and Kundal 2008).

Previous works have dated the bentonitized tuff bands of the Siwalik of Jammu area (Tripathi 1986; Yokoyama *et al.* 1987; Ranga Rao *et al.* 1988; Mehta *et al.* 1993). Tripathi (1986) reported a fission-track age ( $1.6 \pm 0.2$  m.y.) of zircon grains extracted from bentonite band exposed at Uttarbehani section of Nagrota Formation. Subsequently, Yokoyama *et al.* (1987) reported fission-track age of  $1.6 \pm 0.56$  m.y. from zircons recovered from the bentonite band of Barakhetar section. Further, Ranga Rao *et al.* (1988) gave fission-track ages of  $2.8 \pm 0.56$  m.y. and  $2.31 \pm 0.54$  m.y. for bentonite bands of Badakhetar and Nagrota sections, respectively. In conjunction with magnetostratigraphy, Ranga Rao *et al.* (1988) arrived at a conclusion that these bentonite bands straddle across Gauss–Matuyama dated 2.48 m.y. Following this, Mehta *et al.* (1993) reported the fission-track age ( $1.59 \pm 0.32$  m.y.) for the bentonite layer of Badakhetar.

## 2. Methodology

Twelve fresh bentonitized tuff samples (BKB1–BKB12) have been collected for major oxides, trace and rare earth elements. While collecting the samples, weathered surfaces were

avoided and each sample collected after one foot from bottom to top of the bentonitized tuff section. The collected samples were dried in the sunlight and converted into powdered form for geochemical analysis at Wadia Institute of Himalayan Geology, Dehradun. Oxides and trace elemental analyses were carried out by using Standard XRF (Wavelength Dispersive XRF Sequential Spectrometer -WD-XRF) technique, Bruker S8 Tiger. The particle size of the powdered sample is less than 74 micrometer and the quantity of sample was 5–6 gm. The standards used for sediment calibration were USGS (U.S.A.): GXR-2, GXR-5 and the overall accuracy (%RSD) for major oxides was <5% and for trace elements was <12%. The average precision was always better than 1.5%.

For rare earth elements (REE), samples were analyzed by Inductively Couple Plasma-Mass Spectrometer (ICP-MS; PerkinElmer SCIEX ELAN DRC-e) using the open system rock digestion method (Khanna *et al.* 2009). In this method, 100 mg of homogenous powder of each sample (200 mesh) with 10 ml of HF:HNO<sub>3</sub> mixture (2:1) is used. The dried mass of sample in 10 ml of 20% HNO<sub>3</sub> and the standard used for sediment calibration and validation during the analysis was SCo-1, MAG-1, SRG-1 (USGS, USA) the accuracy and precision of Rare earth elements.

### 2.1 Results

The result obtained after geochemical analysis by XRF and ICPMS of bentonitized tuff samples from Badakhetar bentonitized tuff section is given in table 2.

Table 2. Major oxides, trace and rare earth elements data of bentonitized tuff samples (BKB1 to BKB12) from the Badakhetar bentonitized tuff section of Samba district, Jammu province of J&amp;K, India.

Sample no.	BKB1	BKB2	BKB3	BKB4	BKB5	BKB6	BKB7	BKB8	BKB9	BKB10	BKB11	BKB12
Na <sub>2</sub> O%	0.13	0.09	1.16	1.04	1.55	1.78	1.81	1.91	1.88	1.75	1.84	1.64
MgO%	2.82	4.67	2.17	3.26	1.43	0.96	0.87	0.81	0.76	0.94	1.25	1.00
Al <sub>2</sub> O <sub>3</sub> %	23.88	18.96	14.52	14.70	13.28	12.59	12.54	11.73	11.91	12.56	12.23	12.69
SiO <sub>2</sub> %	59.92	63.95	69.77	65.33	70.91	71.59	71.92	70.82	71.13	72.05	69.31	71.27
P <sub>2</sub> O <sub>5</sub> %	0.01	0.00	0.03	0.07	0.03	0.03	0.02	0.04	0.04	0.02	0.06	0.03
K <sub>2</sub> O%	0.19	0.07	2.75	2.40	3.61	4.03	4.09	4.28	4.28	3.98	4.29	3.85
CaO%	1.99	1.83	1.66	2.03	1.50	1.39	1.40	1.39	1.27	1.34	1.51	1.80
TiO <sub>2</sub> %	0.11	0.07	0.23	0.50	0.24	0.22	0.21	0.27	0.25	0.21	0.48	0.22
MnO%	0.07	0.10	0.08	0.08	0.07	0.07	0.07	0.07	0.06	0.06	0.07	0.06
Fe <sub>2</sub> O <sub>3</sub> %	0.90	0.84	1.77	3.39	1.65	1.54	1.47	1.74	1.61	1.49	2.80	1.59
SUM	90.02	90.58	94.14	92.80	94.27	94.20	94.40	93.06	93.19	94.40	93.84	94.15
LOI at 950°C%	25.03	25.30	13.7	13.3	9.95	8.28	8.20	7.37	7.15	8.62	6.75	9.16
LOI at 110°C%	16.90	17.81	8.03	7.85	4.25	2.86	3.00	2.35	2.05	2.93	N.A.	3.02
Ba	421	6	599	501	667	671	704	645	644	720	595	702
Cr	4	BDL	BDL	5	1	BDL	BDL	1	1	1	14	2
V	80	16	23	47	22	20	18	21	21	18	40	19
Sc	6	5	5	3	4	2	3	2	2	1	2	2
Co	18	20	29	18	13	20	18	35	22	33	33	16
Ni	45	29	6	4	2	1	3	1	1	BDL	3	2
Cu	10	14	8	6	6	4	5	5	5	4	8	5
Zn	63	78	84	57	52	48	45	50	51	47	68	47
Ga	34	32	21	20	20	18	17	17	18	18	17	19
Pb	25	41	19	23	22	22	23	21	23	22	19	22
Th	13	8	8	8	6	7	6	6	5	7	8	8
Rb	8	4	97	77	112	122	117	135	135	112	145	112
U	1.1	1	BDL	BDL	2.8	1.5	5.4	BDL	3.4	2.2	1.6	1.3
Sr	143	127	340	216	227	213	207	219	212	207	218	199
Y	5	2	16	14	16	16	16	17	16	16	19	16
Zr	82	62	155	84	89	78	61	92	91	61	130	66
Nb	15	20	12	12	11	11	11	10	11	10	11	10
REE												
La	3.27	1.35	14.12	11.57	9.15	10.98	6.68	8.76	6.14	5.35	7.83	8.27
Ce	10.36	5.55	29.92	25.36	20.62	24.09	19.09	20.53	14.13	14.42	21.04	21.62
Pr	1.00	0.47	3.97	3.27	2.56	3.01	2.14	2.53	1.93	1.51	2.24	2.36
Nd	3.81	1.84	15.76	12.81	10.4	12.03	8.56	10.13	7.9	6.008	8.89	9.26
Sm	1.00	0.5	3.76	3.22	2.71	3.13	2.3	2.64	2.15	1.43	2.11	2.37
Eu	0.23	0.91	0.99	0.82	0.73	0.78	0.65	0.7	0.62	0.44	0.6	0.67
Gd	0.91	0.46	3.33	3.05	2.67	2.96	2.28	2.63	2.16	1.61	2.31	2.4
Tb	0.13	0.06	0.47	0.47	0.41	0.47	0.35	0.4	0.34	0.22	0.33	0.35
Dy	0.68	0.3	2.43	2.59	2.37	2.62	2.05	2.3	1.98	1.19	1.79	1.93
Ho	0.11	0.05	0.42	0.47	0.44	0.5	0.38	0.43	0.37	0.23	0.34	0.36
Er	0.309	0.12	0.99	1.17	1.11	1.23	0.96	1.07	0.95	0.57	0.84	0.9
Tm	0.05	0.02	0.14	0.17	0.16	0.18	0.14	0.16	0.14	0.08	0.12	0.13
Yb	0.48	0.2	0.9	1.19	1.03	1.17	0.91	1.02	0.89	0.56	0.77	0.86
Lu	0.09	0.03	0.13	0.18	0.15	0.15	0.14	0.15	0.13	0.08	0.12	0.13
∑LREE	39.36	18.66	148.5	123.23	99.89	116.46	81.74	97.47	73.1	60.34	88.31	93.31
∑HREE	15.19	6.5	45.18	52.3	44.15	49.1	38.4	43.34	37.14	23.72	34.86	37.26
∑LREE/∑HREE	2.59	2.87	3.28	2.35	2.26	2.37	2.12	2.24	1.96	2.54	2.53	2.50
Eu/Eu*	0.73	0.57	0.85	0.79	0.83	0.78	0.93	0.81	0.87	0.88	0.83	0.85
Ce/Ce*	1.33	1.63	0.93	0.96	0.99	0.98	1.18	1.02	0.96	1.18	1.17	1.14
La/Yb	4.61	4.58	8.03	6.58	6.00	6.35	4.97	5.79	4.67	6.47	6.88	6.51
Gd/Yb	1.53	1.87	3.00	2.07	2.10	2.05	2.03	2.09	1.96	2.33	2.43	2.26

Table 2. (Continued.)

Sample no.	BKB1	BKB2	BKB3	BKB4	BKB5	BKB6	BKB7	BKB8	BKB9	BKB10	BKB11	BKB12
Zr/TiO <sub>2</sub>	0.074	0.088	0.067	0.016	0.037	0.035	0.029	0.034	0.036	0.029	0.027	0.03
La/Y	1.78	1.83	2.40	2.25	1.55	1.86	1.10	1.40	1.04	0.91	1.122	1.40
La/V	0.11	0.22	1.67	0.67	1.13	1.49	1.01	1.13	0.79	0.80	0.53	1.18
Ce/Yb	5.60	7.23	8.63	5.53	5.19	5.34	5.44	5.21	4.12	6.69	7.09	6.52

Note: The above samples are highly hygroscopic and hence the reported LOI is overestimated that includes notable amount of moisture, i.e., H<sub>2</sub>O. BDL: Below detection limit; N.A.: Not available.

### 3. Discussion and interpretation

The original chemical composition of volcanic ash layers is altered by digenesis (Glanzman and Rytuba 1979; Namayandeh *et al.* 2020). Therefore, the types of material/source from which these ash layers were derived cannot be determined from major element data alone as with unaltered glass. For this purpose, whole-rock major, trace and rare earth element geochemistry of bentonitized tuff band was carried out on powdered samples. The obtained geochemical data is used to infer magmatic composition of the parent magma and tectonic setting of the source volcanoes. Many previous studies based on immobile trace and rare earth elements have been carried out in this direction (e.g., Teale and Spears 1986; Merriman and Roberts 1990; Huff *et al.* 1997a, b, 2000; Pattan *et al.* 2001; Nambiar and Sukumaran 2002; Pattan 2002). Some of these studies have generally relied on the use of empirically-based discriminate plots derived from studies of igneous rocks of known origin (e.g., Teale and Spears 1986; Merriman and Roberts 1990; Huff *et al.* 1997a, b, 2000). Although these plots do not provide absolute proof of magma origin or affinity, these plots serve as a useful source of identification of the tectonic settings and general magma chemistry, particularly where other geological evidences are ambiguous (Huff *et al.* 1998). The immobile trace element plots (Zr/TiO<sub>2</sub> vs. Nb/Y) for the bulk ash layers are useful for the classification and inferred the nature of magma. During early alteration, most major elements and many trace elements can be mobile (Floyd and Winchester 1975; Winchester and Floyd 1977; Baragar *et al.* 1979; Gélinas *et al.* 1982), although some plotting using the major elements seem to be useful provided that the analyses are carefully screened and selected before plotting (Pearce 1976; Pearce *et al.* 1977).

#### 3.1 Major oxides

The rocks having high silica content are depleted in MgO and FeO and enriched in Na<sub>2</sub>O and K<sub>2</sub>O. On the other hand, the rocks having low silica content are enriched in MgO and FeO and depleted in Na<sub>2</sub>O and K<sub>2</sub>O. The major oxides and trace elements data of Badakherar bentonitized tuff are listed in table 2. The major oxide (wt%) concentration of 12 samples of Badakhetar bentonitized tuff band is presented in figure 3.

All the samples of bentonitized tuff considerably have high SiO<sub>2</sub> content (59.92–72.05 wt%) with variable Na<sub>2</sub>O (0.09–1.88 wt%), MgO (0.76–4.67%), Al<sub>2</sub>O<sub>3</sub> (11.73–23.88%), P<sub>2</sub>O<sub>5</sub> (0.00–0.07%), K<sub>2</sub>O (0.07–4.29%), CaO (1.27–2.03%), TiO<sub>2</sub> (0.06–0.10%) and Fe<sub>2</sub>O<sub>3</sub> (0.84–3.39%). Samples BKB1, BKB2 and BKB4 have silica content SiO<sub>2</sub> < 66% indicating intermediate nature of bentonitized tuff samples and the samples BKB3, BKB5 to BKB12 have high silica content (SiO<sub>2</sub> > 66%) indicating a felsic nature of the bentonite samples.

Similarly, the range of Na<sub>2</sub>O (0.09–1.04 wt%) and K<sub>2</sub>O (0.07–2.40 wt%) of BKB1–BKB2, and BKB4 is less as compared to Na<sub>2</sub>O (1.16–1.91 wt%) and K<sub>2</sub>O (2.75–4.29 wt%) of BKB3, BKB5 to BKB12. This indicates that BKB3, BKB5 to BKB12 are enriched in Na<sub>2</sub>O and K<sub>2</sub>O, whereas BKB1–BKB2, BKB4 are depleted in Na<sub>2</sub>O and K<sub>2</sub>O.

Al<sub>2</sub>O<sub>3</sub> in BKB1–BKB2, BKB4 ranges from 14.70 to 23.88 wt% which is much higher than BKB3, BKB5–BKB12 (11.73–14.52 wt%). Similarly, CaO in BKB1–BKB2, BKB4 ranges from 1.83 to 2.03 wt% which is higher than that of BKB3, BKB5 to BKB12 (1.27–1.80 wt%). This indicates that with increase in silica content, the CaO content decreases. The BKB1–BKB2, BKB4 have less silica content and high CaO values as compared to BKB3, BKB5–BKB12 which have higher silica content and low CaO values.

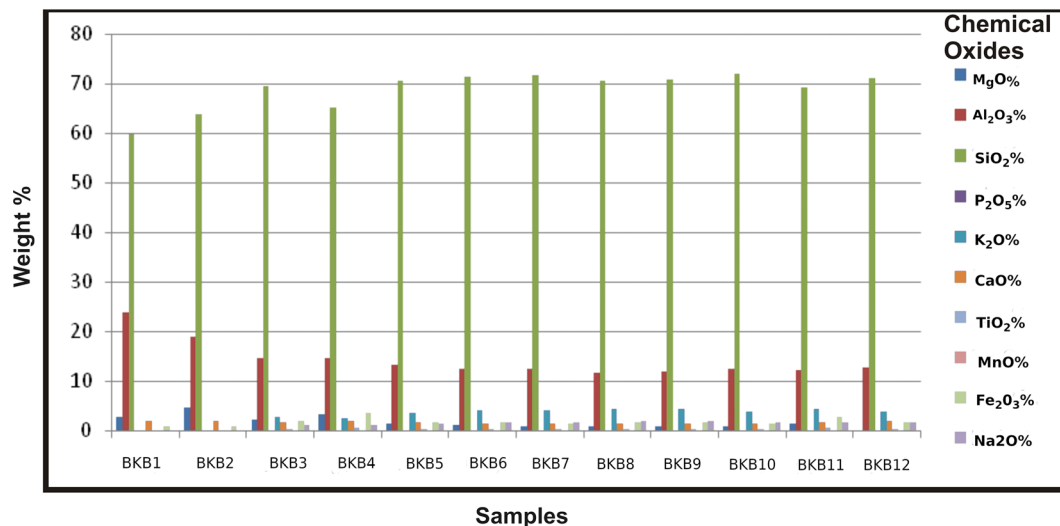


Figure 3. Showing concentration of chemical oxides in bentonitized tuff samples at Badakhetar, Jammu province.

The alkali content of the BKB1, BKB2 and BKB4 was much smaller than BKB3, BKB5–BKB12 samples, indicating a major loss of alkalis during alteration (e.g., Senkayi *et al.* 1984; Shiraki *et al.* 1987; Altaner and Grim 1990; Christidis and Scott 1997). The relatively higher  $K_2O$  and  $Na_2O$  contents of BKB3, BKB5–BKB12 of the bentonitized tuff samples reflect the presence of authigenic K-feldspar and mordenite, respectively.

### 3.2 Trace elements

The high field strength elements like Zr, Nb, Hf, Ta and rare earth elements and  $TiO_2$  are commonly considered to be immobile under most conditions of diagenesis and low-grade metamorphism and thus are useful indicators of petrogenetic processes (Huff *et al.* 1998). The Nb/Y ratio is widely used as a measure of alkalinity and Zr/ $TiO_2$  ratio as an index of differentiation. Izett (1981) concluded that many explosively erupted volcanic ashes tend to have moderate to high Nb and Zr content reflective of their silicic and high volatile ( $H_2O$ ) character. The Zr/ $TiO_2$  vs.  $SiO_2$  (wt%) and Zr/ $TiO_2$  vs. Nb/Y chemical discrimination diagrams (Winchester and Floyd 1977) are used for the classification of bentonites.

Samples BKB1–BKB12 plotted on Zr/ $TiO_2$  vs.  $SiO_2$  (wt%) classification diagram (figure 4) resulted in a range from rhyodacite to trachyandesite with  $SiO_2$  between 59.92 and 72.05 wt%. In bentonitized tuffs/clay, Si tetrahedral shows least variation of major elements and has a

mean value relative to continental crust of nearly one.

Similarly, BKB1 to BKB12 are plotted on Zr/ $TiO_2$  vs. Nb/Y diagram (figure 5). The Zr/ $TiO_2$  vs. Nb/Y suggests derivation from felsic magma having trachyte, trachyte–andesite and andesitic affinity. The high Zr/ $TiO_2$  ratio (0.01–0.08) also suggests trachyte–andesite composition for the bentonitized tuff samples. The low Nb, Th and Zr values are suggestive of subalkaline origin for these samples.

The trace elemental data has also been plotted on several widely referred discrimination plots to reveal the tectomagmatic origin of altered volcanic ashes. Immobile elements Y (ppm) and Nb (ppm) values of bentonitized samples (BKB1–BKB12) are plotted on a discrimination diagram (after Pearce *et al.* 1984) (figure 6). All the samples of bentonitized tuff band plot in the fields of Volcanic Arc Granites Plus Syn-Collision tectomagmatic setting (VAG + Syn-COLG). This indicates that the source of Badakhetar bentonitized tuff band was Volcanic Arc Granite + Syn Collision tectomagmatic setting.

#### 3.2.1 La/Th vs. Th/Yb

The La/Th vs. Th/Yb plots have been used to differentiate between felsic and mafic nature of source rocks (Bhatia and Crook 1986). The La/Th ranges between 0.168 and 1.765 and Th/Yb values between 5.042 and 40.0 of 12 samples of bentonitized tuff band from Badakhetar section has been plotted on La/Th vs. Th/Yb plots (figure 7).



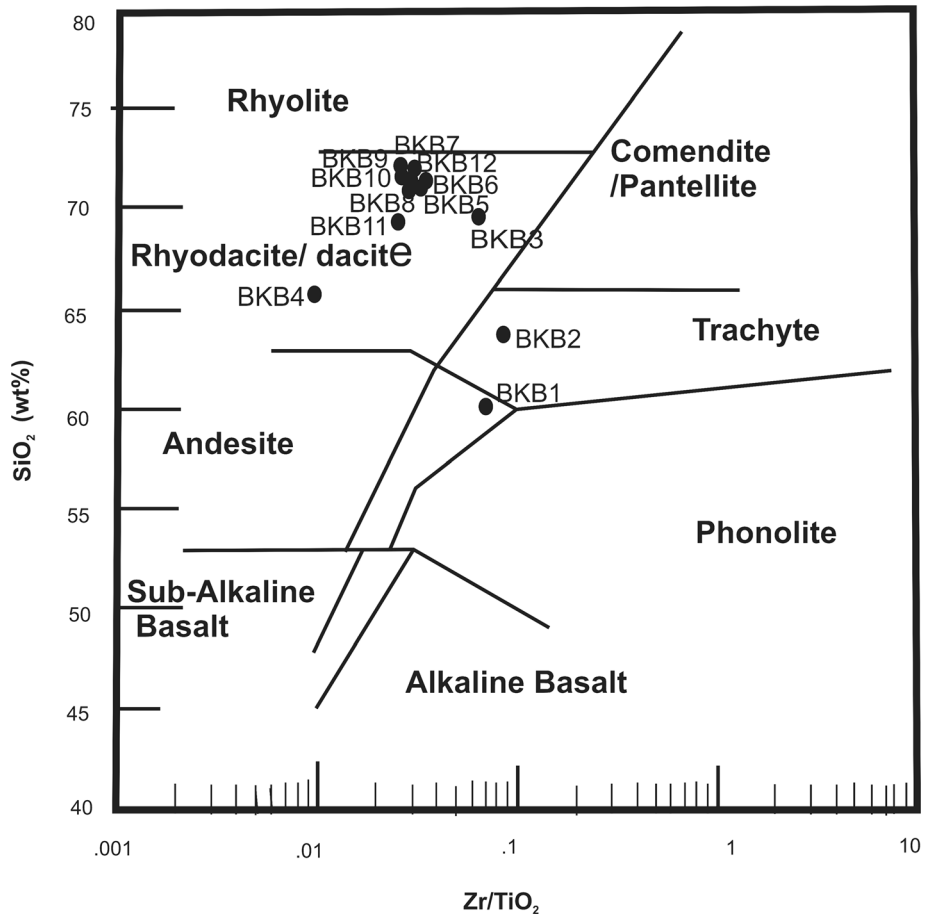


Figure 4. Zr/TiO<sub>2</sub> vs. SiO<sub>2</sub> (wt%) classifying studied samples as rhyodacite to trachyandesite with an SiO<sub>2</sub> range of 59.92–72.05 wt% (Winchester and Floyd 1977).

BKB3–BKB12 shows felsic character of source rock by its unusual high La/Th (felsic provenance) as compared with samples (BKB1 and BKB2) having low La/Th value and high Th/Yb value (intermediate provenance).

### 3.3 Rare earth elements

#### 3.3.1 Chondrite normalized plot

The chondrite normalized values (Taylor and McLennan 1985) of rare earth elements for 12 bentonitized tuff samples from Badakhetar section are plotted on the spider diagram (figure 8). All the samples show negative sloping curves with an overall increase in light rare earth elements of 4–17 times chondritic and heavy rare earth elements by a factor of 1–3. These observations are characteristic of a calc-alkaline nature magmas of subduction related to volcanic arc

environments (Taylor and McLennan 1988; McVey and Huff 1995).

#### 3.3.2 Degree of fractionation elements

Degree of fractionation/fractionation indices of rare earth elements can be expressed by  $La_{\text{chondrite normalized}}/Yb_{\text{chondrite normalized}}$ . It is an index of the concentration of light rare earth elements (La or Ce) over heavy rare earth elements (Yb). A combination of  $La_{\text{chondrite normalized}}/Yb_{\text{chondrite normalized}}$  ratio with Eu anomaly plays a measure role to describe the rare earth elements pattern and is very useful to determine the source rock. The  $La_{\text{chondrite normalized}}/Yb_{\text{chondrite normalized}}$  values of 12 samples (BKB1–BKB12) are within the range of 4.58 and 8.03 with an average 5.95 suggests that the light rare earth elements are enriched with respect to heavy rare earth elements.

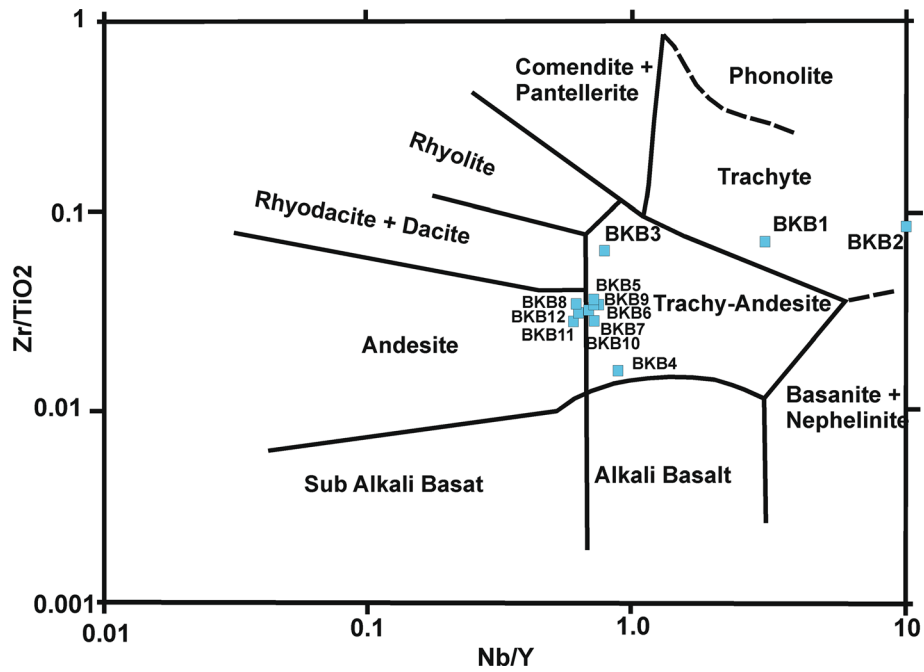


Figure 5. Bentonitized tuff band range from andesite to trachyandesite to trachyte with range Zr/TiO<sub>2</sub> between 0.01 and 0.08 and Nb/Y between 0.57 and 10.

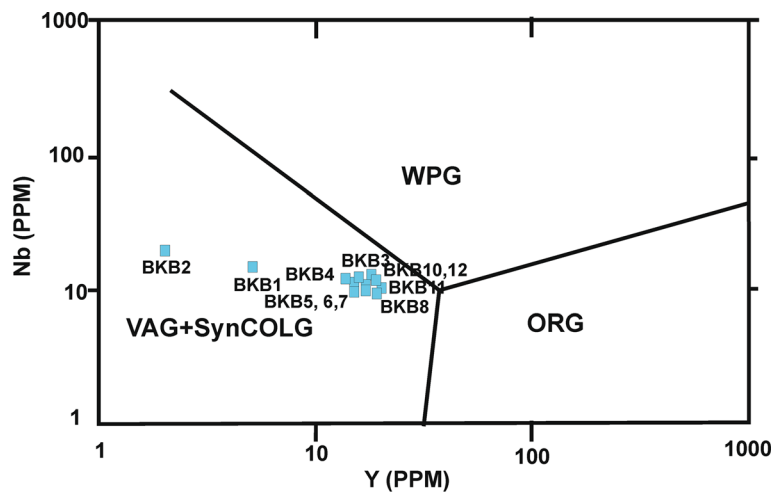


Figure 6. Y (ppm) and Nb (ppm) values of bentonitized tuff samples (BKB1–BKB12) plotted on the discriminate diagram (after Pearce *et al.* 1984) indicating volcanic arc granites plus syn-collision tectomagmatic setting (VAG + Syn-COLG) source of bentonitized tuff band.

### 3.3.3 Europium (Eu) anomaly

The past events that existed in the reducing igneous environment (events occurred in upper continental crust) can be indicated by anomalous activity of Eu.

Europium anomaly (Eu anomaly) is generally represented by Eu/Eu\* and can be expressed (Liao *et al.* 2016) as:

$$Eu/Eu^* = \frac{Eu_{\text{chondrite normalized}}}{0.5 \times Sm_{\text{chondrite normalized}} \times 0.5 \times Gd_{\text{chondrite normalized}}}$$

In felsic rocks, plagioclase majorly controls the Eu anomaly. The Eu/Eu\* values >0.85 indicate a positive Eu anomaly while Eu/Eu\* values <0.85 indicate a negative Eu anomaly and values =0.85 indicate no anomaly.

The Eu anomaly of the bentonitized tuff band samples ranges between 0.56 and 0.93 with an average of 0.81 suggesting a negative Eu anomaly. Individual Eu anomaly values of 0.73 (BKB1), 0.57 (BKB2), 0.79 (BKB4), 0.83 (BKB5), 0.78 (BKB6), 0.81 (BKB8) and 0.83 (BKB11) is <0.85 which also corresponds to negative Eu anomaly, sample

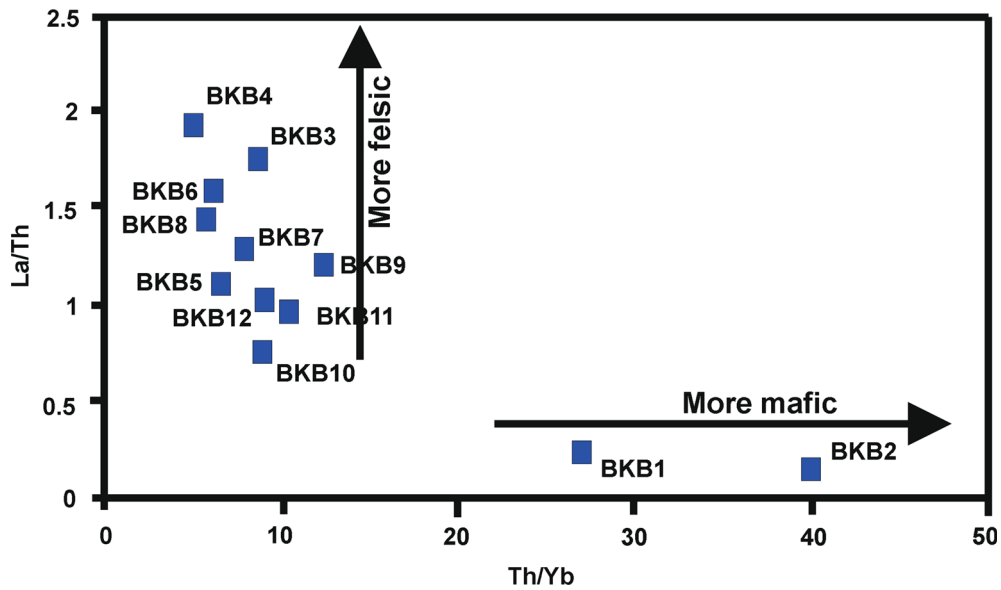


Figure 7. La/Th vs. Th/Yb plot (Bhatia and Crook 1986) indicating BKB1–BKB2 intermediate provenance and BKB3–BKB12 indicating felsic provenance.

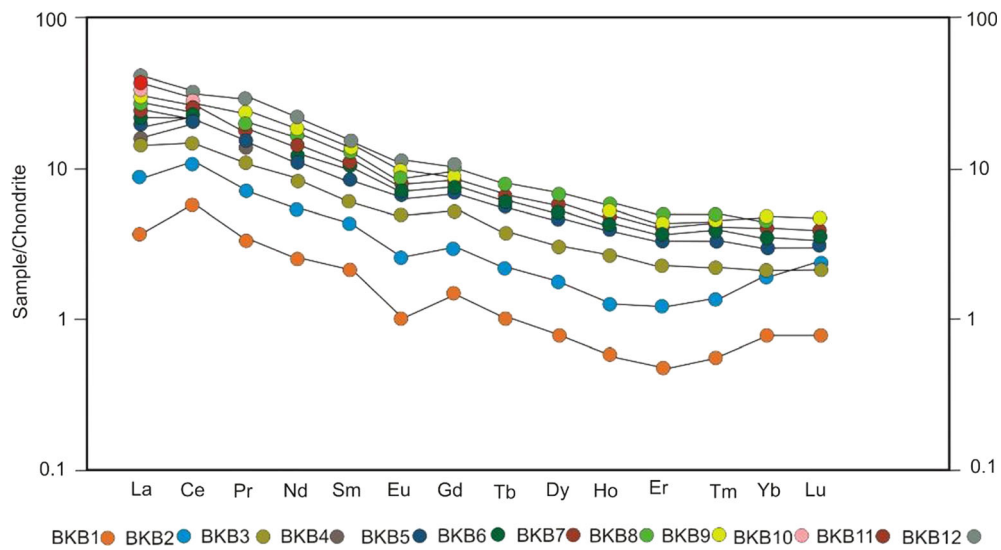


Figure 8. Chondrite-normalized REE patterns of 12 bentonitized tuff band samples of Badakhetar section showing slightly enrichment of LREE over HREE during the alteration processes (chondrite normalizing values are from Taylor and McLennan 1985).

BKB12 (0.85) and BKB3 (0.85) corresponding to no Eu anomaly and sample BKB7 (0.93), BKB9 (0.87) and BKB10 (0.88) >0.85 indicate slightly positive Eu anomaly. The negative Eu anomaly is usually in felsic rocks and sediments due to intracrustal fractionation/lithospheric/weathering of feldspar and a positive Eu anomaly is due to the origin of feldspar or prominent areas affected in hydrothermal vents (Rudnick 1992). The LREE/HREE ratio in felsic rocks is usually high and more pronounced to negative Eu anomaly while LREE/

HREE ratio in mafic rocks is usually low and a few or no Eu anomalies.

### 3.3.4 Cerium (Ce) anomaly

Cerium anomaly is the concentration of Cerium in rock either enriched or depleted relative to other rare earth elements. If Cerium is depleted in a rock relative to other REE, the Ce anomaly is said to be negative and if the Cerium is enriched in a rock relative to other REE, the Ce anomaly is said to be

positive. This only occurs in the marine environmental condition associated with the formation of nodulus (manganese). In marine conditions, when  $Ce^{3+}$  oxides to  $Ce^{4+}$ , it separates as an insoluble phosphate. The result is distinctive Ce depletion in marine water conditions.

Cerium anomaly (Ce anomaly) is generally represented by  $Ce/Ce^*$  and expressed as:

$$\frac{Ce/Ce_{\text{chondrite normalized}}^*}{0.5 \times La_{\text{chondrite normalized}} \times 0.5 \times Pr_{\text{chondrite normalized}}} = \frac{Ce_{\text{chondrite normalized}}}{0.5 \times La_{\text{chondrite normalized}} \times 0.5 \times Pr_{\text{chondrite normalized}}}$$

$Ce/Ce_{\text{chondrite normalized}}^*$  bentonitized tuff samples (BKB1–BKB12) from Badakhshar range from 0.93 to 1.63 with an average value 1.12 indicating a positive Ce anomaly, but individual Ce anomaly values of samples BKB1–BKB2, BKB7–BKB12 ranges from 1.02 to 1.63 indicating a positive Ce anomaly and that of samples BKB3–BKB5, BKB9 ranges from 0.93 to 0.97 indicate a negative Ce anomaly.

The REE pattern of the samples clearly indicates enrichment of LREEs over HREEs with higher Ce/Yb ratios. This is quite similar to the REE content of most of the fine-grained sedimentary rocks. The sample BKB3, BKB5–BKB12 is showing further higher enrichment of LREEs suggesting a very high percentage of clays with very low biogenic carbonate and quartz. The chondrite normalized plot is showing a negative Eu anomaly. The negative anomaly is commonly observed in all the sedimentary rocks. The only important sedimentary rock type with no Eu depletion is the first cycle volcanogenic sediments deposited in forearc basins of Island arcs and derived mainly from andesites (Nauce and Taylor 1977).

The negative Eu anomaly in the present study may be due to the chemical fractionation and represent a reducing environment. The negative Ce anomaly is not a common phenomenon of the fine-grained sedimentary rocks; it may be due to chemical weathering in the acidic environment (Brown *et al.* 1955). Alternatively, these Ce and Eu anomalies may represent the source from rhyolitic/rhyodacitic to trachyandesitic composition, which is more plausible in the present case. Furthermore, diagenetic changes in Eh also affect Ce and Eu because of their ability to exist in different oxidation states under geological conditions. A pronounced negative Eu anomaly in some samples indicates earlier crystallization of plagioclase (e.g., Huff *et al.* 1998). The lack of corresponding depleted HREE indicates the fractionation of

phases such as garnet and clinopyroxene, did not play a major role in the evolution of these calc-alkaline magmas. In addition, a very slightly negative Ce and Er anomalies in all the samples suggest depletion due to diagenesis in an alkaline environment. A pronounced positive Tm anomaly is attributed to contribution from the facies and the alkaline depositional environment. The bentonitized tuff band samples have unique chemical signatures in having euhedral biotite and apatite grains and less abundant zircons and possess high field strength elements such as Zr, Y, Th and Nb. The uncommon zircon combined with the presence of apatite crystals and weak Eu anomaly implies that the source was not an oversaturated peralkaline melt (MacDonald and Spooner 1981).

Vitroclastic texture or even relic primary volcanic glass, phenocrysts such as clear quartz, sanidine, plagioclase, pyroxene, euhedral biotite, euhedral zircon, apatite and their distinct morphological feature, clay mineral assemblage all indicate that the Upper Siwalik bentonitized tuff band is derived from altered volcanic ash. Variations in colour and composition indicate that the layers may be comprised of several eruptions.

### 3.4 Degree of weathering

To check the degree of weathering of a parent rock, it is essential to know element mobility during the change of volcanic tuff to bentonite. To understand the geochemical characteristics of source rock, physical reworking intensity and changes of igneous rocks, the felsic volcanic rocks ratio of  $TiO_2/Al_2O_3$  has been widely used (Zhou and Kyte 1988; Burger *et al.* 2002; He *et al.* 2014; Hong *et al.* 2019). The most immobile elements during the devitrification of volcanic ash to authigenic bentonite are Al and Ti (Slack and Stevens 1994; Hong *et al.* 2019). Ti has more mobility than Al which results in diminishing the  $TiO_2/Al_2O_3$  ratio progressively with increasing intensity of weathering. Hong *et al.* (2019) calculated the  $TiO_2/Al_2O_3$  values and classified the degree of weathering for felsic volcanic rocks are as under (i) if the  $TiO_2/Al_2O_3$  ratio is  $<0.055$ , it corresponds to primary ash compositions, (ii) if the  $TiO_2/Al_2O_3$  ratio is between 0.055 and 0.140, it suggests a moderate degree of weathering, and (iii) if  $TiO_2/Al_2O_3$  ratio is  $>0.140$ , it suggests strong degree of weathering.

All the samples of bentonitized tuff from the Badakhetar section possess  $TiO_2/Al_2O_3$  ranging between 0.0001 and 0.0230 with an average value of 0.01341 indicating primary ash composition/original composition of rock. Eu anomaly is commonly used to know the composition of source magma and is not influenced by reworking.  $Eu/Eu^*$  vs.  $TiO_2/Al_2O_3$  is used to evaluate the reworking effect during the deposition of ash. All the samples are plotted on  $Eu/Eu^*$  vs.  $TiO_2/Al_2O_3$  diagram that further highlights primary volcanic tuff nature near the composition of rhyolite/rhyodacite (figure 9).

#### 4. Source of bentonitized tuff band

During the Plio-Pleistocene times, there is no evidence of volcanic activity in north India. The presence of volcanic ash bed or bentonitized tuff band in the entire region of the Upper Siwalik of Jammu area suggests that the volcanic activity might have taken place during Plio-Pleistocene times. This band is extended up to Pinjor in Himachal Pradesh towards northeast in India and towards northwest, it extends into Pakistan and Afghanistan. In Pakistan, Johnson *et al.* (1982) identified the bentonitized tuff band and tuffaceous mudstones at four stratigraphic levels and these levels show variation in composition, which

indicates multi-volcanic activity that took place during Plio-Pleistocene times.

The Dasht-e-Nawar volcanic complex of east-central Afghanistan (Pliocene–Quaternary centre for volcanism) has several large strato volcanoes, explosion centres with associated welded tuff, and explosion breccia and domes which are primarily andesites and rhyodacites. These are 50 independent volcanoes known in Dasht-e-Nawar area, but few are dated (Johnson *et al.* 1982). These rocks are composed of andesites, with cusped and platy quartz shards, rhyodacites and lamprophyres having pyroxene, hornblende, fine microlites of feldspars, glass with gas cavities, pumice, biotite, sphene, apatite, zircon, tourmaline, etc.

The ash particles have blown with wind and cover approximately 1000 km distance. The bigger size and dense ash particles fall near to the source (near the place of eruption) and the small size and light ash particles were swept away from the source. The high sp. gravity ash particles settle down on the earth surfaces earlier than the low sp. gravity ash particles (e.g., the tuffaceous mudstone beds occurred at the base and composed of dark gray coloured of heavy minerals). The low sp. gravity and light-coloured minerals occurred above the tuffaceous mudstone and show grading towards top.

The present study points to the possibility that the bentonitized tuff band of Jammu might be the product

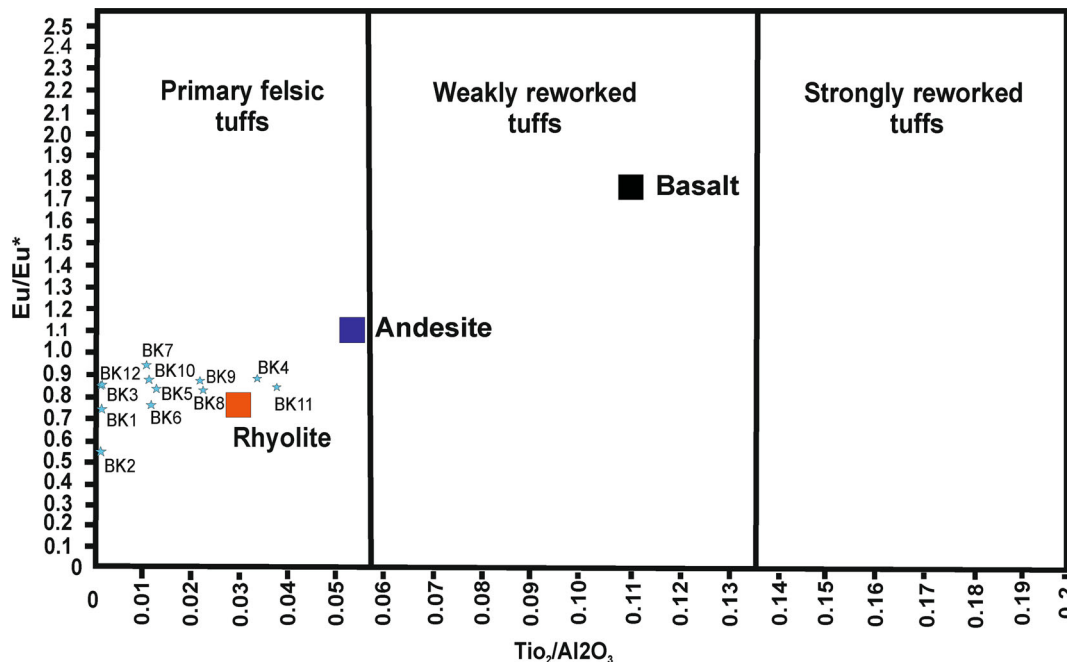


Figure 9.  $TiO_2/Al_2O_3$  vs.  $Eu/Eu^*$  discriminate diagram parent rocks (blue star) (Hong *et al.* 2019). Rhyolite (in red square), andesite (in blue square) and basalt data (in Black Square) are from Laviano and Mongelli (1996). All the samples (BKB1–BKB12) fall in the domain of primary felsic tuffs.

of the volcanic activity that has taken place in Dasht-e-Nawar volcanic complex. This interpretation is based on the following three grounds: (1) The composition of Jammu bentonitized tuff band is same as that of Dasht-e-Nawar volcanic complex, (2) the time of deposition of the Jammu bentonitized tuff band and the eruption time of Dasht-e-Nawar volcanic complex is same, i.e., Plio-Pleistocene, and (3) the bentonitized tuff band has been reported in detached outcrops from Pakistan through Jammu and Kashmir to Himachal Pradesh at the same stratigraphic level.

## 5. Conclusion

Geochemistry of bentonitized tuff band from the Jammu area reveals their intermediate to felsic nature and their affinity towards rhyodacite–trachyandesite–andesite. Tectonic discrimination diagrams reveal volcanic arc granite plus syn-collisional tectonic setting. Chondrite normalized REE values indicate slight enrichment of LREE over HREE. Eu anomaly ranges from 0.56 to 0.93 indicating a mix of both positive and negative Eu anomaly.  $TiO_2/Al_2O_3$  values of samples are  $<0.055$  suggesting their primary ash compositions.  $TiO_2/Al_2O_3$  vs.  $Eu/Eu^*$  values suggest no reworking effect during deposition of bentonitized tuff band. The Dasht-e-Nawar volcanic complex of east-central Afghanistan might be the source of bentonitized tuff band of Jammu province. Variation in colour and grain size from bottom to top in different laminae indicates episodic eruption.

## Acknowledgements

The corresponding author is thankful to the Science and Engineering Research Board, New Delhi for financial support under research project (SR/FTP/ES-71/2013) through which the samples were analyzed at Wadia Institute of Himalayan Geology, Dehradun, India. He also thanks Prof Pankaj Srivastava, Department of Geology, University of Jammu for helping them during the interpretation of the geochemical data. Also, the authors are thankful to Prof N V Chalapathi Rao, Editor, Earth System Science for closely reviewing and editing the manuscript.

## Author statement

SNK interpreted the geochemical data and prepared the manuscript. NC collected the bentonite

samples from the field and prepared them for geochemical analysis. SK did the computational work of the manuscript including preparation of figures.

## References

- Agarwal R P, Nanda A C, Prasad D N and Dey B K 1993 Geology and biostratigraphy of the Upper Siwalik of Samba area, Jammu foothills; *Him. Geol.* **4**(2) 227–236.
- Altaner S P and Grim R E 1990 Mineralogy, chemistry, and diagenesis of tuffs in the Sucker Creek Formation (Miocene), eastern Oregon; *Clays Clay Miner.* **38**(6) 561–572.
- Arif M, Mazhar F, Mujeeb-ur-Rahman and Ullah R 2005 Mineralogy and chemistry of volcanic clay (fuller's earth) from Taunsa area, Dera Ghazi Khan, Pakistan; *J. Him. Earth Sci. Abstracts.*
- Arslan M, Kadir S, Abdioglu E and Kolayli H 2006 Origin and formation of kaolin minerals in saprolite of Tertiary alkaline volcanic rocks, Eastern Pontides, NE Turkey; *Clay Miner.* **41**(2) 597–617.
- Baragar W R A, Plant A G, Pringle G J and Schau M 1979 Diagenetic and post-diagenetic changes in the composition of an Archean pillow; *Can. J. Earth Sci.* **16**(11) 2102–2121.
- Barr S M and Cooper M A 2013 Late Cenozoic basalt and gabbro in the subsurface in the Phetchabun Basin, Thailand: Implications for the Southeast Asian Volcanic Province; *J. Asian Earth Sci.* **76** 169–184.
- Batchelor R A 2014 Geochemistry of Upper Ordovician metabentonites and their cognates apatite microphe-nocrysts from Norway and Sweden; *GFF* **136**(2) 87–397.
- Bhandari A and Kundal S N 2008 Ostrocodes from the Nagrota Formation, Upper Siwalik Subgroup, Jammu, India; *Rev. Espanolla de Micropaleontol.* **40**(1–2) 151–166.
- Bhat G M, Kundal S N, Pandita S K and Prasad G V R 2008 Depositional origin of tuffaceous units in the Pliocene upper Siwalik Subgroup, Jammu (India), NW Himalaya; *Geol. Mag.* **145**(2) 279–294.
- Bhatia M R and Crook K A 1986 Trace element characteristics of graywackes and tectonic setting discrimination of sedimentary basins; *Contrib. Mineral. Petrol.* **92**(2) 181–193.
- Bhola K L 1948 Bentonite in India; *Quart. J. Geol. Min. Metal. Soc. India* **19** 55–77.
- Brown R E, Parker H M and Smith J M 1955 Disposal of liquid wastes to the ground; In: *UN Int. Conf. on the Peaceful uses of Atomic Energy*, United Nations, New York, pp. 669–675.
- Burbank D W and Tahirkheli R K 1985 The magnetostratigraphy, fission-track dating, and stratigraphic evolution of the Peshawar intermontane basin, northern Pakistan; *Geol. Soc. Am. Bull.* **96**(4) 539–552.
- Burger K, Zhou Y and Ren Y 2002 Petrography and geochemistry of tonsteins from the 4th Member of the Upper Triassic Xujiahe formation in southern Sichuan Province, China; *Int. J. Coal Geol.* **49**(1) 1–17.
- Caballero E, De Cisneros C J, Huertas F J, Huertas F, Pozzuoli A and Linares J 2005 Bentonites from Cabo de Gata, Almeria, Spain: A mineralogical and geochemical overview; *Clay Miner.* **40**(4) 463–480.
- Christidis G E 1998 Physical and chemical properties of some bentonite deposits of Kimolos Island, Greece; *Appl. Clay Sci.* **13**(2) 79–98.

- Christidis G and Dunham A C 1997 Compositional variations in smectites: Part II. Alteration of acidic precursors, a case study from Milos Island, Greece; *Clay Miner.* **32**(2) 253–270.
- Christidis G E and Huff W D 2009 Geological aspects and genesis of bentonites; *Elements* **5**(2) 93–98.
- Christidis G E and Scott P W 1997 The origin and control of colour of white bentonites from the Aegean islands of Milos and Kimolos, Greece; *Mineral. Depos.* **32**(3) 271–279.
- Christidis G E, Scott P W and Marcopoulos T 1995 Origin of the bentonite deposits of Eastern Milos, Aegean, Greece: Geological, mineralogical and geochemical evidence; *Clays Clay Miner.* **43**(1) 63–77.
- Edani M, Meunier A, Zahraoui M D, Beaufort M, El Wartiti, Fontaine C, Boukili B and El Mah B 2005 Clay mineralogy and chemical composition of bentonites from the Gourougou volcanic massif (northeast Morocco); *Clays Clay Miner.* **53**(3) 250–267.
- Eliyas N, Khan N, Kumar D, Singh P, Prakash S, Kumar R and Singh R J 2017 Siwalik Group of northwest Sub-Himalaya; *Workshop on Indian Siwalik: Recent Advances and Future Research*, GSI Northern region, Lucknow, pp. 181–205.
- Elliott H, Wall F, Chakhmouradian A R, Siegfried P R, Dahlgren S, Finch S, Weatherley A A, Marks M A W, Dowman E and Deady E 2018 Fenites associated with carbonatite complexes: A review; *Ore Geol. Rev.* **93** 38–59.
- Fisher R V and Schmincke J U 1984 *Pyroclastic rocks*; Springer-Verlag, Berlin, 465p.
- Floyd P A and Winchester J A 1975 Magma type and tectonic setting discrimination using immobile element; *Ore Geol. Rev.* **27**(2) 211–218.
- Ge X, Mou C, Wang C, Men X, Chen C and Hou Q 2019 Mineralogical and geochemical characteristics of K-bentonites from the Late Ordovician to the Early Silurian in South China and their geological significance; *Geol. J.* **54**(1) 514–528.
- Gélinas L, Mellinger M and Trudel P 1982 Archean mafic metavolcanics from the Rouyn–Noranda district, Abitibi Greenstone Belt, Quebec. 1: Mobility of the major elements; *Can. J. Earth Sci.* **19**(12) 2258–2275.
- Glanzman R K and Rytuba J J 1979 Zeolite-clay mineral zonation of volcanoclastic sediments within the McDermitt Caldera Complex of Nevada and Oregon; U.S. Geological Survey Open-File Report 79-1688; U.S. Geological Survey: Menlo Park, CA, USA, 25p.
- Göncüoğlu M C, Günel-Türkmenoğlu A, Bozkaya Ö, Ünlüce-Yücel Ö, Okuyucu C and Yılmaz İ Ö 2016 Geological features and geochemical characteristics of Late Devonian–Early Carboniferous K-bentonites from northwestern Turkey; *Clay Miner.* **51**(4) 539–562.
- Gupta L N 1996a A re-appraisal of tuffaceous mudstone from Upper Siwalik sequences of Pinjor region; *Ind. Mineral.* **30** 11–19.
- Gupta L N 1996b Evaluation of reported ash beds from Upper Siwalik basins of India and Pakistan; *Pub. Centre Adv. Study in Geol. Panjab University, Chandigarh* **5** 17–38.
- Gupta S S 2000 Lithostratigraphy and structure of the Siwalik succession and its relationship with the Muree succession around Ramnagar area, Udhampur district, Jammu and Kashmir; *Him. Geol.* **21** 53–61.
- Gupta L N and Kochhar N 2002 Ash beds in the northwestern Himalayan; *J. Geol. Soc. India* **59** 485–486.
- Gupta S S and Verma B C 1988 Stratigraphy and vertebrate fauna of the Siwalik Group, Jammu District, Mansar–Uttarbarani section, Jammu and Kashmir; *J. Palaeontol. Soc. India* **33** 117–124.
- Gupta L N, Dhar B L and Kochhar N 1999 A comment on ash bed of Jammu region; (Abstract) *XVI - Convention Indian Assoc. Sedimentol.*, University of Jammu.
- Gupta L N, Kumar R and Gill G S 2001 A comparison of petrochemical characters of the reported ash beds from the Upper Siwalik Formation of India; *Structure and Tectonic of the Indian Plate*, pp. 153–170.
- He B, Zhong Y, Xu Y and Li X 2014 Triggers of Permian–Triassic boundary mass extinction in South China: The Siberian Traps or Paleo-Tethys ignimbrite flare-up?; *Lithos* **204** 258–267.
- Hong Y, Wang L, Yang B and Zhang J 2019 Stress-dilatancy behaviour of bubbled fine-grained sediments; *Eng. Geol.* **260** 105–196.
- Huff W D, Bergstrom S M, Kolata D R and Sun H 1997a The Lower Silurian Osmundsberg K-bentonite. Part II: Mineralogy, geochemistry, chemostratigraphy and tectonomagmatic significance; *Geol. Mag.* **135**(1) 15–26.
- Huff W D, Morgan D J and Rundle C C 1997b Silurian K-bentonites of the Welsh Borderlands: Geochemistry, mineralogy and K–Ar ages of illitization; *British Geol. Surv. Report* WG/96/45, 25.
- Huff W D, Bergstrom S M, Kolata D R and Sun H 1998 The Lower Silurian Osmundsberg K-bentonite. Part-II: Mineralogy, geochemistry, chemostratigraphy and tectonomagmatic significance; *Geol. Mag.* **135** 15–26.
- Huff W D, Bergstrom S M and Kolata D R 2000 Silurian K-bentonite of the Dnestr basin, Podolia, Ukraine; *J. Geol. Soc. London* **157** 493–504.
- Izett G A 1981 Volcanic ash beds: Recorders of Upper Cenozoic silicic pyroclastic volcanism in the western United States; *J. Geophys. Res.* **86** 1020–1022.
- Johnson G D, Zeitler P, Naesser C W, Johnson N M, Summers D M and Frost C D 1982 The occurrence and fission track ages of late Neogene and volcanic sediments, Siwalik Group Northern Pakistan; *Palaeogeogr. Palaeoclimatol. Palaeoecol.* **37** 63–93.
- Khanna P P, Saini N K, Mukherjee P and Purohit K K 2009 An appraisal of ICP-MS technique for determination of REEs: Long term QC assessment of silicate rock analysis; *Him. Geol.* **30**(1) 95–99.
- Kiipli T, Dahlqvist P, Kallaste T, Kiipli E and Nolvak J 2015 Upper Katian (Ordovician) bentonites in the East Baltic, Scandinavia and Scotland: Geochemical correlation and volcanic source interpretation; *Geol. Mag.* **152**(4) 589.
- Kundal S N 2013 Late Pliocene (Piacenzian Stage) fossil Molluscs from Upper Siwalik Subgroup of Jammu, Jammu and Kashmir, India; *Int. Res. J. Earth Sci.* **1**(4) 10–17.
- Kundal S N 2015 Microfossils based palaeoecology and palaeocommunity structure of Upper Siwalik Deposits of Jammu, J and K, India; *Int. Res. J. Biol. Sci.* **4**(1) 34–40.
- Kundal S N 2018 *Mus* cf. *Mus flynni* (Rodentia, Mammalia) from mudstone horizon underlying ash beds, Upper Siwalik of Samba District, Jammu and Kashmir, India; *Arab. J. Geosci.* **11** 474.

- Kundal S N, Bhadur G and Kumar S 2017 *Elephas cf. planifrons* (Elephantidae, Mammalia) from Upper Siwalik Subgroup of Samba district, Jammu and Kashmir, India; *Vertebrata Palasiatica* **55(1)** 59–70.
- Kundal S N, Bhat G M, Pandita S K and Ahmed M 2011 Field observations, mineralogical composition and XRD analysis of bentonitized tuff band, Jammu Province, Jammu and Kashmir, India; *Int. J. Develop. Studies* **5(1)** 77–86.
- Kundal S N, Bhat G M, Prasad G V R and Pandita S K 1999 Origin, sedimentological and geochemical characteristics of the Upper Siwalik bentonite band, Jammu; *XVI Convention, Indian Association of Sedimentology*, pp. 18–19.
- Laviano R and Mongelli G 1996 Geochemistry and mineralogy as indicators of parental affinity for Cenozoic bentonites: A case study from S. Croce di Magliano (Southern Apennines, Italy); *Clay Miner.* **31(3)** 391–401.
- Liao Z, Hu W, Ca J, Wang X, Yao S, Wu H and Wan Y 2016 Heterogeneous volcanism across the Permian–Triassic Boundary in South China and implications for the latest Permian Mass Extinction: New evidence from volcanic ash layers in the lower Yangtze Region; *J. Asian Earth Sci.* **127** 197–210.
- MacDonald R 1987 Quaternary peralkaline silicic rocks and caldera volcanoes of Kenya; In: *Alkaline Igneous Rocks* (eds) Fitton J G and Upton B G J, *Geol. Soc. London, Spec. Publ.* **30** 313–333.
- MacDonald A J and Spooner E T C 1981 Calibration of a Linkam TH 600 programmable heating cooling stage for micro-thermometric examination of fluid inclusions; *Econ. Geol.* **76(5)** 1248–1258.
- McLennan S M 1989 Rare earth elements in sedimentary rocks: Influence of provenance and sedimentary processes; *Geochem. Miner. REE Rev. Mineral.* **21** 169–200.
- McLennan S M 2001 Relationships between the trace element composition of sedimentary rocks and upper continental crust; *Geochem. Geophys. Geosyst.* **2(4)**.
- McVey D E and Huff W D 1995 Southern and central Appalachian stratigraphy interpreted with the use of the Middle Ordovician Deicke and Millbrig K-bentonite beds; In: *Ordovician Odyssey: Short papers for the Seventh International Symposium on the Ordovician System* (eds) Cooper J D, Droser M L and Finney S C, The Pacific Section Society for Sedimentary Geology Book 77, 351p.
- Mehta Y P, Thakur A K, Lal N, Shukla B and Tandon S K 1993 Fission track age of zircon separates of tuffaceous mudstones of the Upper Siwalik Subgroup of Jammu-Chandigarh sector of the Punjab Sub-Himalaya; *Curr. Sci.* **64(7)** 519–521.
- Merriman R J and Roberts B 1990 Metabentonites in the Moffat shale group, southern uplands of Scotland: Geochemical evidence of ensialic marginal basin volcanism; *Geol. Mag.* **127(3)** 259–271.
- Middlemiss C S 1930 Jammu and Kashmir Minerals Survey Report, pp. 32–37.
- Namayandeh A, Modabberi S and López-Galindo A 2020 Trace and rare earth elements distribution and mobility during diagenetic alteration of volcanic ash to bentonite in Eastern Iranian bentonite deposits; *Clays Clay Miner.* **68** 50–66.
- Nambiar A R and Sukumaran P V 2002 Characterisation of Late Pleistocene tephra in deep sea sediments of Arabian sea; *J. Geol. Soc. India* **59** 79–88.
- Nauce W B and Taylor S R 1977 Rare earth element patterns and crustal evolution-II. Arcsedimentary rocks from Kalgoorlie, Australia; *Geochim. Cosmochim. Acta* **41(2)** 225–231.
- Opdyke N D, Lindsay E, Johnson G D, Johnson N M, Tahirkeleli R A K and Mirza M A 1979 Magnetic polarity stratigraphy and vertebrate palaeontology of Upper Siwalik Subgroup of northern Pakistan; *Palaeogeogr. Palaeoclimatol. Palaeoecol.* **27** 1–34.
- Pattan J N 2002 Volcanic ash and its enigma: A case study from the central Indian Ocean basin; *J. Geol. Soc. India* **60** 127–130.
- Pattan J N, Shane P, Pearce N J G, Banakar V K and Parthiban G 2001 An occurrence of the 74 ka youngest Toba tephra from the western continental margin of India; *Curr. Sci.* **80** 1322–1326.
- Pearce J A 1976 Statistical analysis of major element patterns in basalts; *J. Petrol.* **17(1)** 15–43.
- Pearce T H, Gorman B E and Birkett T C 1977 The relationship between major element chemistry and tectonic environment of basic and intermediate volcanic rocks; *Earth Planet. Sci. Lett.* **36(1)** 121–132.
- Pearce J A, Harris N B and Tindle A G 1984 Trace element discrimination diagrams for the tectonic interpretation of granitic rocks; *J. Petrol.* **25(4)** 956–983.
- Pilgrim G E 1934 Correlation of fossiliferous section in Upper Cenozoic of India; *Amer. Mus. Novitates* **704** 1–5.
- Pozo M, Carretero M I and Galán E 2016 Approach to the trace element geochemistry of non-marine sepiolite deposits: Influence of the sedimentary environment (Madrid Basin, Spain); *Appl. Clay Sci.* **131** 27–43.
- Prasad G V R, Kundal S N and Bhat G M 2005 Mandible of *Golunda* (Rodentia, Mammalia) from the Upper Siwalik Subgroup of Jammu, India; *Ann. Paleontol.* **91** 81–96.
- Ranga Rao A, Agarwal R P, Sharma U N, Bhalla M S and Nanda A C 1988 Magnetic polarity stratigraphy and vertebrate palaeontology of the Upper Siwalik Subgroup of Jammu Hills India; *J. Geol. Soc. India* **31** 361–385.
- Rudnick R L 1992 Restites, Eu anomalies and the lower continental crust; *Geochim. Cosmochim. Acta* **56(3)** 963–970.
- Senkayi A L, Dixon J B, Hossner L R, Abder-Ruhman M and Fanning D S 1984 Mineralogy and genetic relationships of tonstein, bentonite, and lignitic strata in the Eocene Yegua Formation of east-central Texas; *Clays Clay Miner.* **32(4)** 259–271.
- Shiraki R, Sakai H, Endoh M and Kishima N 1987 Experimental studies on rhyolite and andesite seawater interactions at 300 C and 1000 bars; *Geochem. J.* **21(4)** 139–148.
- Siritongkham N, Srichan W, Khositantont S and Limtrakun P 2020 Mineralogy, geochemistry and genesis of bentonite deposits in Lam Narai volcanic belts, Lop Buri province, central Thailand; *S. N. Appl. Sci.* **2(5)** 946, <https://doi.org/10.1007/s42452-020-2755-7>.
- Slack J F and Stevens B P 1994 Clastic metasediments of the early Proterozoic Broken Hill group, new South Wales, Australia: Geochemistry, provenance and metallogenic significance; *Geochim. Cosmochim. Acta* **58(17)** 3633–3652.
- Sorkhabi R B and Macfarlane A 1999 Himalaya and Tibet: Mountain roots to mountain tops; In: *Himalaya and Tibet: Mountain roots to mountain top* (eds) Macfarlane A,



- Sorkhabi R B and Quade J, Geological Society of America, special paper **328** 1–7.
- Tandon S K and Kumar R 1984 Discovery of tuffaceous mudstones in the Pinjor formation of Punjab sub-Himalaya, India; *Curr. Sci.* **53(18)** 982–984.
- Taylor S R and McLennan S M 1985 *The continental crust: Its composition and evolution*; Blackwell Scientific Publications, Oxford, 312p.
- Taylor S R and McLennan S M 1988 The significance of rare earths in geochemistry and cosmochemistry; In: *Handbook on the physics and chemistry of rare earths* (eds) Gschneider K A and Eyring L, Elsevier, New York, pp. 485–578.
- Teale C T and Spears D A 1986 The mineralogy and origin of some Silurian bentonites, Welsh Borderland, United Kingdom; *Sedimentology* **33** 757–765.
- Tripathi C 1986 Siwalik of the Indian sub-continent; *J. Palaeontol. Soc. India* **31** 1–8.
- Ullah R, Nie Fengjuin N, Zhang Xin Z, Zhang Chengyong Z, Izha S, Idrees Safdar I and Ali A 2020 Occurrence of a likely tuff bed between the middle and upper Siwaliks, Taunsa area, Dera Ghazi Khan, eastern Sulaiman range, Pakistan; *Int. J. Econ. Environ. Geol.* **11(1)** 24–34.
- Verma B C, Mishra V P and Gupta S S 2002 Pictorial catalogue of Siwalik vertebrate fossils from northwest Himalaya; *Geological Survey of India* **5** 1–378.
- Visser C F and Johnson G D 1978 Tectonic control of late Pliocene molasse sedimentation in a portion of the helum re-entrant Pakistan; *Sonderdruck aus der geologischen Rundschau Ban* **67** 15–37.
- Winchester J A and Floyd P A 1977 Geochemical discriminations of different magma series and their differentiation. Products using immobile elements; *Chem. Geol.* **20** 325–343.
- Yalcin H and Gumuser G 2000 Mineralogical and geochemical characteristics of Lat Cretaceous bentonite deposits of the Kelkit Valley Region, Northern Turkey; *Clay Mineral.* **35(5)** 807–825.
- Yokoyama T, Verma B C, Mastuda T, Gupta S S and Tewari A P 1987 Fission-track age of a bentonitized ash bed and mammalian fauna from Nagrota Formation (Upper Siwalik) of Jammu District (J & K), India; *Ind. Mineral.* **41(4)** 13–23.
- Zhou L and Kyte F T 1988 The Permian–Triassic boundary event: A geochemical study of three Chinese sections; *Earth Planet. Sci. Lett.* **90(4)** 411–421.

Corresponding editor: N V CHALAPATHI RAO